



HAL
open science

Time domain analysis and localization of a non-local PML for dispersive wave equations

Nacéra Baara, Julien Diaz, Mounir Tlemcani

► **To cite this version:**

Nacéra Baara, Julien Diaz, Mounir Tlemcani. Time domain analysis and localization of a non-local PML for dispersive wave equations. *Journal of Computational Physics*, 2021, 445, pp.110638. 10.1016/j.jcp.2021.110638 . hal-03523312

HAL Id: hal-03523312

<https://inria.hal.science/hal-03523312v1>

Submitted on 12 Jan 2022

HAL is a multi-disciplinary open access archive for the deposit and dissemination of scientific research documents, whether they are published or not. The documents may come from teaching and research institutions in France or abroad, or from public or private research centers.

L'archive ouverte pluridisciplinaire **HAL**, est destinée au dépôt et à la diffusion de documents scientifiques de niveau recherche, publiés ou non, émanant des établissements d'enseignement et de recherche français ou étrangers, des laboratoires publics ou privés.

Time domain analysis and localization of a non-local PML for dispersive wave equations

Nacéra BAARA^a, Julien DIAZ^b, Mounir TLEMCANI^{a,*}

^a*Université des Sciences et Technologies d'Oran - Mohamed Boudiaf (USTOMB) Algérie*

^b*Project-team Magique-3D, Inria, Université de Pau et des Pays de l'Adour, CNRS, France*

Abstract

In this work we design and analyze new perfectly matched layers (PML) for a dispersive waves equation : the Klein Gordon equation. We show that because of the dispersion, classical PMLs do not guarantee the convergence to zero of the error, which hampers the precision in long time simulation. We propose to consider a non-local PML for which we can obtain explicit uniform estimates for the reflected analytical solution in time domain, given by an integral representation formula. This uniform estimates ensure the convergence of the error to zero at fixed time t and guarantee the accuracy of the layer. For the implementation of the new PML, we propose a localization technique that we validate numerically.

Keywords: Klein-Gordon equation, PML, dispersion, analytical solution, Green's function, Bessel's functions, uniform error, long time stability.

2000 MSC: 35L05, 35L10, 35L20, 35A08, 35A22

1. Introduction

2 Evolution of gravity waves in the Navier-Stokes, Euler or shallow water equa-
3 tions when rotation is taken into account may propagate waves at different
4 speeds not proportional to their wavelengths. Such a phenomena is called dis-
5 persion and is described by a parameter α in the present work. Dispersion may
6 also be seen as the wave number in higher (three dimensions for instance) *via*
7 a Fourier transform w.r.t. the third variable in space which leads in particu-
8 lar to common procedures for constructing absorbing boundary conditions for
9 wave-like equations. We will present in this work new ideas to deal numerically
10 with some problems of wave propagation in an unbounded dispersive medium
11 for which we have chosen the Klein-Gordon equation as the standard model of
12 the dispersive wave equation. The results presented in this paper are useful for
13 authors who are interested in the dynamics of large-scale motions of the oceans
14 and atmosphere in geophysical rotating fluid dynamics, cf. eg. [24].

*Corresponding author: mounir.tlemcani@gmail.com

15 Since Bérenger [8, 9], the Perfectly Matched Layer (PML) technique was in-
16 troduced as an alternative for the absorbing boundary condition (ABC) method
17 (cf. Engquist [17, 18]) to simulate the propagation of waves in unbounded do-
18 mains. It consists in truncating the computational domain by an absorbing
19 layer with a damping term acting only in the orthogonal direction for outgoing
20 waves and having the nice property that the layer is perfectly matched at the
21 interface. In computational codes, the most crucial drawback of PML's imple-
22 mentation is a stability property of the associated equations in the layer for long
23 time simulation of the total wave field (transmitted plus reflected).

24 While existing results mainly concern modal or plane wave analysis for the
25 question of stability in time domain analysis (cf. eg. [12, 1, 6]), explicit error
26 estimates were discussed in the literature by very few authors. We refer to [16]
27 for a detailed presentation in the case of advective acoustics in time domain
28 with parallel mean flow. To the authors' knowledge, no such results exist for
29 dispersive waves such as for example Klein-Gordon equation or more generally
30 damped waves with dispersion.

31 Based on the Cagniard-de Hoop method [13, 10, 14, 25], known for its power
32 in the case of stratified media, the authors in [16] have obtained analytical solu-
33 tion and explicit error estimates for PMLs for advective acoustics which result
34 from the linearized Euler system. Because of the lack of homogeneity of some
35 integrand functions in the Fourier-Laplace space, the method does not apply
36 (at least straightforwardly) if one considers the dispersion term in designing
37 PMLs for wave problems as in rotating shallow water [20, 2, 5], in particu-
38 lar for Klein-Gordon wave like equations. In our study, we propose to replace
39 the Laplace variable, denoted by s , by a non-local one $\sqrt{s^2 + \alpha^2}$ specifically
40 including Bessel's functions when returning back to time-domain solutions [3].
41 Doing so, one takes into account the dispersion term denoted by α implicitly
42 in such a way that the new forms of the equations will correspond exactly to
43 a non-dispersive case. Thanks to this new variable, we present in this work an
44 integral representation of the Green's function associated with the Klein Gordon
45 equation. This expression can be derived explicitly and therefore the analytical
46 solution follows by a convolution in time with the source term. A new non-local
47 PML formulation is deduced and can consequently be analyzed in time-domain
48 in a very similar way to that of [16]. We refer to [26, 12, 9, 11] (the list is not
49 exhaustive) for more details on PMLs in time domain acoustics. Recently, the
50 authors in [7] have shown the failure of standard PML change of variable for
51 some dispersive cases such as the Drude model in electromagnetics. They have
52 proposed a modification of the time frequency ω by $\omega\psi(\omega)$ where $\psi(\omega)$ is a suit-
53 able rational function of ω that ensures the stability of the absorbing layer. In
54 our study, we present a localization technique for a particular dispersive model
55 in acoustics (the Klein-Gordon equation) that allows us to build such functions
56 in order to ensure both the stability and the precision of the PML for long
57 waves adjustment. As a main result, explicit error estimates are obtained for
58 the non-local PML's formulation associated to the Klein-Gordon equation (i.e.,
59 dispersive waves), long time stability results still hold but uniform convergence
60 result to zero of the error failed when the time goes to infinity. In addition, a

61 new PML based on a localization technique is proposed and shown to be better
 62 than the classical one for inertial oscillations regime that is specific to dispersive
 63 waves solutions.

64 In the second section, we present the main steps of constructing non-local
 65 PMLs for dispersive wave like equations in two dimensions. The third section
 66 is devoted to the computation of fundamental solution in whole (free) space
 67 (the incident Green's function) and in a half space with PML of finite width
 68 (the reflected Green's function). These fundamental solutions allow us to obtain
 69 the analytical solution of the PML's equation as a convolution (in the sense of
 70 Laplace transform) of the total field (Green's function) with the source term
 71 located in space in the physical domain. We present a fundamental lemma that
 72 permits us to write a representation formula for the fundamental solution via
 73 Bessel's functions and the Green's function of the non-dispersive wave equation.
 74 This provides a splitting of the solution as a non-dispersive part and a purely
 75 dispersive one. In the fourth section, error estimates are obtained in a very
 76 similar way to that of [16] by taking care on the behaviour for long time of an
 77 oscillating integral appearing in the dispersive part of the solution. As a result,
 78 the uniform error does not converge to zero in long time because of a term
 79 proportional to $\sqrt{\alpha}$ appearing in the upper bound, explaining therefore the fact
 80 that long time stability is conserved but the precision can be justified at most
 81 for small α . In the fifth section, a localization technique at high frequencies is
 82 presented similarly to the ABC's methodology [17] and a numerical comparison
 83 of the zeroth and first order Taylor approximations of the square root $\sqrt{\partial_t^2 + \alpha^2}$
 84 is performed. Numerical experiments are thus presented in order to validate the
 85 effect of α on designing PMLs for dispersive waves, particularly for long waves
 86 regime which arises after very long periods in time. The last section is devoted
 87 to conclusions, comments and remarks.

88 2. Non-local PML for a family of 2d dispersive wave equations

89 Let us consider the two-dimensional family of dispersive wave equations

$$\frac{1}{c^2} \frac{\partial^2}{\partial t^2} u_\alpha - \Delta u_\alpha + \alpha^2 u_\alpha = f(x, t), \quad x = (x_1, x_2) \in \mathbb{R}^2, \quad t > 0, \quad (1)$$

90 where $\alpha \geq 0$ is the so-called dispersion parameter. For simplicity and without
 91 restriction, we will assume in all what follows that $c = 1$. If the initial data of
 92 the problem is compactly supported in the domain of interest $\mathbb{R}_-^2 = \mathbb{R}_- \times \mathbb{R}$,
 93 then it is natural to reduce computation to this left half-space. There are two
 94 main classes of methods to do so. The first ones consist in approximating
 95 the radiation condition at finite distance resulting in the so-called absorbing
 96 boundary conditions (ABC). The second ones are called perfectly matched layers
 97 (PML) and consist in adding a fictitious layer that at the same time adapts the
 98 impedance at the interface and absorbs the outgoing waves, cf. Figure 1. As
 99 this method is furthermore really easy to implement (specifically in the corners
 100 of the domain), it has rapidly attracted a lot of people in different fields of
 101 application.

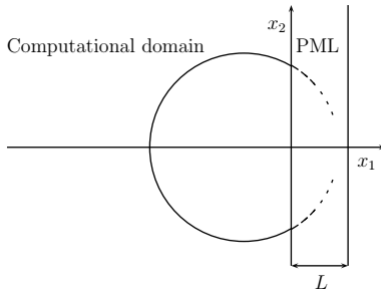


Figure 1: Computational domain and Perfectly Matched Layer

102 When $\alpha = 0$, and alternatively to the original idea of Bérenger (1996), PML
 103 can be implemented by adding a layer of width L in which (1) is modified via
 104 an absorption term $\sigma \geq 0$ by replacing the x_1 -spatial derivative $\frac{\partial}{\partial x_1}$ in (1) by

$$D_{x_1}^\sigma = \left(\frac{\partial}{\partial t} + \sigma(x_1) \right)^{-1} \frac{\partial}{\partial t} \frac{\partial}{\partial x_1}. \quad (2)$$

105 In the present work, we propose to extend this change of variable in such a
 106 way that both perfect matching and good stability properties of the layer are
 107 conserved exactly as in the case $\alpha = 0$, i.e. without dispersion. In fact, we can
 108 achieve this at the expense of the local character of the PML as follows: the
 109 x_1 -spatial derivative $\frac{\partial}{\partial x_1}$ in (1) will be replaced rather by (at least formally)

$$D_{x_1, \alpha}^\sigma = \left(\sqrt{\frac{\partial^2}{\partial t^2} + \alpha^2} + \sigma(x_1) \right)^{-1} \sqrt{\frac{\partial^2}{\partial t^2} + \alpha^2} \frac{\partial}{\partial x_1}, \quad (3)$$

110 in such a way that $D_{x_1, 0}^\sigma$ coincides with the standard $D_{x_1}^\sigma$. The second order
 111 formulation of the PML (a vertical layer of width L) reads as follows:

$$\left(\frac{\partial^2}{\partial t^2} + \alpha^2 \right) u_\alpha - (D_{x_1, \alpha}^\sigma)^2 u_\alpha - \frac{\partial^2}{\partial x_2^2} u_\alpha = 0, \quad x = (x_1, x_2) \in (0, L) \times \mathbb{R}, t > 0. \quad (4)$$

112 It is well known that the homogeneous equation associated to (1) supports plane
 113 wave solutions proportional to $e^{i(\omega t - \mathbf{k} \cdot \mathbf{x})}$ where ω and $\mathbf{k} = (k_1, k_2)^t$ designate the
 114 time frequency and wave vector respectively. These two parameters are related
 115 by the so-called dispersion relation $-\omega^2 + \mathbf{k}^2 + \alpha^2 = 0$ where $k := \sqrt{k_1^2 + k_2^2}$
 116 denotes the wave number. As shown in Figure 2, dispersive waves have a cut-off
 117 frequency at $\omega = \alpha$ that corresponds to inertial oscillations and appears after
 118 very long periods in time. The major difference between dispersive and non-
 119 dispersive waves can be located in the vicinity of this cut-off frequency, while
 120 for k large there is no significant distinction. It is precisely with the aim of
 121 correctly taking into account the modes close to inertial oscillations that we are
 122 led to consider the idea of non-local PMLs.

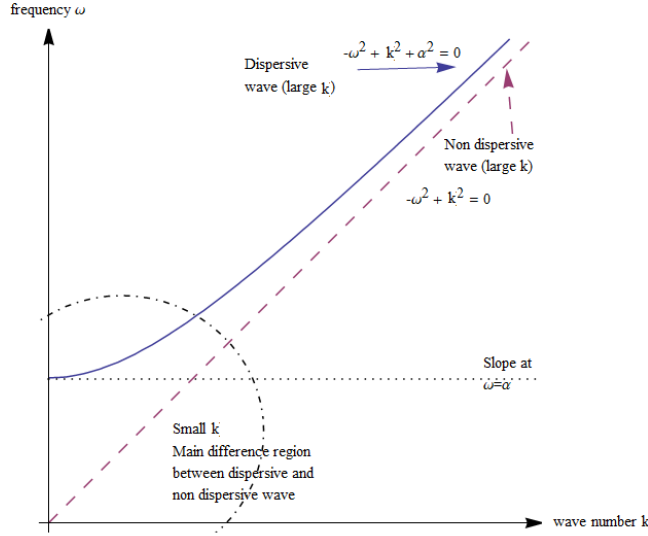


Figure 2: Dispersion relation of the KG equation in the cases $\alpha \neq 0$ (dispersive waves) and $\alpha = 0$ (non-dispersive waves).

123 We are thus interested in the following transmission problem with a regular
 124 point source $f(t)$ compactly supported in $[0, T)$ and located in space at $x_S =$
 125 $(-h, 0) \in \mathbb{R}_* \times \mathbb{R}$ and an absorption profile $\sigma \equiv \sigma(x) > 0$ if $0 < x < L$ (L may
 126 be finite or not) and $\sigma \equiv 0$ if $x \leq 0$,

$$\left\{ \begin{array}{l} \text{Find } u_{\alpha}^{\sigma, L} : (-\infty, L) \times \mathbb{R} \times \mathbb{R}_+ \rightarrow \mathbb{R}, \text{ zero for } t < 0, \\ \left(\frac{\partial^2}{\partial t^2} + \alpha^2 \right) u_{\alpha}^{\sigma, L} - (D_{x_1, \alpha}^{\sigma})^2 u_{\alpha}^{\sigma, L} - \frac{\partial^2 u_{\alpha}^{\sigma, L}}{\partial x_2^2} = \delta(x - x_S) f(t), \\ u_{\alpha}^{\sigma, L} \Big|_{x_1 \rightarrow 0^-} = u_{\alpha}^{\sigma, L} \Big|_{x_1 \rightarrow 0^+}, \\ \frac{\partial u_{\alpha}^{\sigma, L}}{\partial x_1} \Big|_{x_1 \rightarrow 0^-} = D_{x_1, \alpha}^{\sigma} u_{\alpha}^{\sigma, L} \Big|_{x_1 \rightarrow 0^+}, \\ \frac{\partial u_{\alpha}^{\sigma, L}}{\partial x_1} \Big|_{x_1 = L} = 0, \quad \text{if } L < +\infty. \end{array} \right. \quad (5)$$

127 Of course, the solution is assumed to be a causal and tempered distribution with
 128 support in $(-\infty, L) \times \mathbb{R} \times \mathbb{R}^+$. In the third and fourth lines of (5) we recognize
 129 the perfect matching conditions at the interface $x_1 = 0$ and in the last equation
 130 we chose a Neumann-type condition at the outer boundary $x_1 = L$. Notice that
 131 one can choose a condition of Dirichlet-type instead of Neumann with a slight
 132 change in the principle of the image to determine the analytical solution in the
 133 case of a finite layer.

134 **3. Integral representation of the Green's function**

135 Following results that are presented in [16] in the case of a dispersionless
 136 media (i.e. $\alpha = 0$) with full details based on the Cagniard de-Hoop method for
 137 obtaining analytical solutions, one can deduce fundamental (Green's function)
 138 and analytical solutions associated to Problem (5). Fundamental solutions are
 139 those that correspond to $f(t) = \delta(t)$.

140 Let us define the two coordinate systems, $(r, \theta) \in \mathbb{R}_+ \times (0, 2\pi]$, such that
 141 $x - x_S = (r \cos \theta, r \sin \theta)^t$, which is relative to the point source $x_S = (-h, 0)$
 142 and $(r^*, \theta^*) \in \mathbb{R}_+ \times (\pi/2, 3\pi/2]$ such that $x - x_S^* = (r^* \cos \theta^*, r^* \sin \theta^*)^t$, which
 143 is relative to the image point source $x_S^* = (h + 2L, 0)$, symmetrical to x_S w.r.t.
 144 the line $x_1 = L$, as shown in Figure 3. More precisely, one has $r^*(x) = r(x^*)$
 145 and $\theta^*(x) = \theta(x^*)$ where x^* is the image of $x = (x_1, x_2)$ by the transformation
 $x^* = (2L - x_1, x_2)$. For $\sigma \equiv \sigma(x_1) > 0$ if $x_1 > 0$ and $\sigma \equiv 0$ if $x_1 \leq 0$, with the

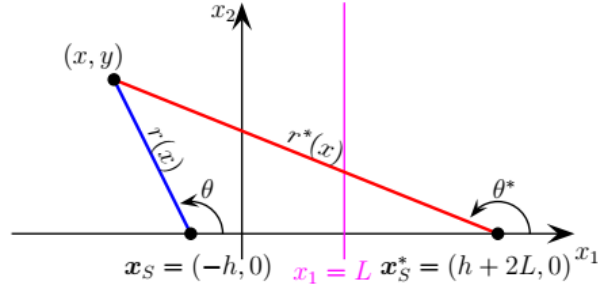


Figure 3: Coordinate system w.r.t. x_S and x_S^* .

146 notation $\Sigma(x_1) = \int_0^{x_1} \sigma(x) dx$, let us also define the functions

$$A(x, t) = |\cos \theta(x)| \Sigma(x_1) \frac{t}{r(x)}, \quad B(x, t) = |\sin \theta(x)| \Sigma(x_1) \sqrt{\frac{t^2}{r(x)^2} - 1}.$$

148 Then, we have:

- 149 • In the case of an infinite layer ($L = +\infty$), $G_i^{\sigma, \infty}(x, t) = G_{\alpha=0, i}^{\sigma, \infty}(x, t)$ the
 150 fundamental solution of Problem (5) in a dispersionless media (i.e., for
 151 $\alpha = 0$) is given by, cf. [16, Theorem 1],

$$G_i^{\sigma, \infty}(x, t) = \frac{H(t - r(x))}{2\pi \sqrt{t^2 - r(x)^2}} e^{-A(x, t)} \cos[B(x, t)], \quad x_1 \in \mathbb{R}.$$

- 152 • In the case of a finite layer ($L < +\infty$), the expression of the fundamental
 153 solution $G^{\sigma, L}(x, t)$ of Problem (5) in a dispersionless media is such that

$$G^{\sigma, L}(x, t) = G_i^{\sigma, \infty}(x, t) + G_i^{\sigma, \infty}(x^*, t), \quad (6)$$

154 where we have extended σ symmetrically w.r.t. the line $x_1 = L$ as

$$\sigma(x_1) = \begin{cases} \sigma(x_1) & \text{if } -\infty < x_1 < L, \\ \sigma(2L - x_1) & \text{if } L < x_1 < +\infty. \end{cases}$$

The second term in the r.h.s. of (6),

$$G_i^{\sigma, \infty}(x^*, t) := G_r^{\sigma, L}(x, t)$$

155 is called the reflected field and admits the following expression, cf. [16,
156 Theorem 3],

$$G_r^{\sigma, L}(x, t) = \frac{H(t - r(x^*))}{2\pi\sqrt{t^2 - r(x^*)^2}} e^{-A(x^*, t)} \cos[B(x^*, t)], \quad x_1 \in \mathbb{R}.$$

157 The above results were obtained mainly in [16] with the help of the so-called
158 Cagniard-de Hoop method which gives, handling some complex contours, a di-
159 rect inversion formula for the Fourier-Laplace transform of $G_i^{\sigma, \infty}$ in the space
160 variable x_2 and time t ,

$$\tilde{G}_i^{\sigma, \infty}(x_1, k, s) = \frac{e^{-\sqrt{k^2 + s^2} |x_1 + h + \frac{\Sigma(x_1)}{s}|}}{2\sqrt{k^2 + s^2}}, \quad s > 0. \quad (7)$$

161

162 **Lemma 1.** Let $\tilde{G}_\alpha(s)$ the Laplace transform of a causal function $G_\alpha(t)$, $\alpha \in$
163 \mathbb{R}_+ , such that

$$\tilde{G}_\alpha(s) = \tilde{G}_0(\sqrt{s^2 + \alpha^2}), \quad (8)$$

164 then $G_\alpha(t)$ has the following integral representation

$$G_\alpha(t) = G_0(t) - \alpha \int_0^t G_0(\sqrt{t^2 - z^2}) J_1(\alpha z) dz, \quad (9)$$

165 where J_ν ($\nu \in \mathbb{Z}$) denotes the Bessel function of the first kind.

166 **Proof.** Direct consequence of the following inverse Laplace transform formula
167 cf. [4, p.p. 248 – (23)],

$$\mathcal{L}^{-1}\left(e^{-hs} - e^{-h\sqrt{s^2 + \alpha^2}}\right) = \frac{\alpha h J_1(\alpha\sqrt{t^2 - h^2})}{\sqrt{t^2 - h^2}} H(t - h),$$

168 which yields

$$\mathcal{L}^{-1}\left(e^{-h\sqrt{s^2 + \alpha^2}}\right) = \delta(t - h) - \frac{\alpha h J_1(\alpha\sqrt{t^2 - h^2})}{\sqrt{t^2 - h^2}} H(t - h),$$

169 δ and H being respectively the Dirac and Heaviside functions. In fact, by
 170 causality of G_0 and linearity of \mathcal{L}^{-1} applied to (8), one obtains

$$\begin{aligned}
 G_\alpha(t) &= \mathcal{L}^{-1} \left(\int_0^{+\infty} G_0(t') e^{-t' \sqrt{s^2 + \alpha^2}} dt' \right), \\
 &= \int_0^{+\infty} G_0(t') \mathcal{L}^{-1} \left(e^{-t' \sqrt{s^2 + \alpha^2}} \right) dt', \\
 &= \int_0^{+\infty} G_0(t') \delta(t - t') dt' - \int_0^{+\infty} G_0(t') \frac{\alpha t' J_1(\alpha \sqrt{t^2 - t'^2})}{\sqrt{t^2 - t'^2}} H(t - t') dt', \\
 &= G_0(t) - \int_0^t G_0(t') \frac{\alpha t' J_1(\alpha \sqrt{t^2 - t'^2})}{\sqrt{t^2 - t'^2}} dt',
 \end{aligned}$$

171 which gives (9), using the change of variable $z = \sqrt{t^2 - t'^2}$ in the last integral.

172 ■

Theorem 1. *The expression of the fundamental solution $G_\alpha^{\sigma,L}(x, t)$ of Problem (5) for $\alpha \geq 0$ is given by*

$$G_\alpha^{\sigma,L}(x, t) = G_{\alpha,i}^{\sigma,\infty}(x, t) + G_{\alpha,r}^{\sigma,L}(x, t), \quad (10)$$

173 where $G_{\alpha,r}^{\sigma,L}(x, t) = 0$ if $L = +\infty$, and

$$G_{\alpha,r}^{\sigma,L}(x, t) = G_{\alpha,i}^{\sigma,\infty}(x^*, t) \quad \text{if } L < +\infty, \quad (11)$$

174 $G_{\alpha,r}^{\sigma,L}(x, t)$ is the reflected field and $G_{\alpha,i}^{\sigma,\infty}(x, t)$ is the incident field and is related
 175 to the dispersionless incident field $G_i^{\sigma,\infty}(x, t)$ by the following representation
 176 formula:

$$G_{\alpha,i}^{\sigma,\infty}(x, t) = G_i^{\sigma,\infty}(x, t) - \alpha \int_0^t G_i^{\sigma,\infty}(x, \sqrt{t^2 - z^2}) J_1(\alpha z) dz. \quad (12)$$

177 **Proof.** Let us start computing a fundamental solution for an infinite layer,
 178 i.e. $L = +\infty$. We let $f(t) = \delta(t)$ and to simplify the notation let us denote $G_\alpha^{\sigma,L}$
 179 by G_α . Taking a Laplace-Fourier transform in time t and space x_2 , $G_\alpha(\cdot, x_2, t) \mapsto$
 180 $\tilde{G}_\alpha(\cdot, k, s)$, in the partial differential equation in Problem (5), the function $x_1 \mapsto$
 181 $\tilde{G}_\alpha(x_1, k, s)$ satisfies the following ordinary differential equation with variable
 182 coefficients:

$$(s^2 + \alpha^2 + k^2) \tilde{G}_\alpha - \left(\tilde{D}_{x_1, \alpha}^\sigma \right)^2 \tilde{G}_\alpha = \delta(x_1 + h), \quad (13)$$

183 where

$$\tilde{D}_{x_1, \alpha}^\sigma = \left(\sqrt{s^2 + \alpha^2} + \sigma(x_1) \right)^{-1} \sqrt{s^2 + \alpha^2} \frac{d}{dx_1}.$$

184 We now use the change of variable

$$X_1(x_1, s) = x_1 + \frac{1}{\sqrt{s^2 + \alpha^2}} \int_0^{x_1} \sigma(x) dx,$$

185 and we introduce the new unknown \mathcal{G}_α such that

$$\tilde{\mathcal{G}}_\alpha(X_1(x_1, s), k, s) = \tilde{G}_\alpha(x_1, k, s).$$

186 We get for $x_1 > 0$,

$$\frac{d\tilde{\mathcal{G}}_\alpha}{dX_1} = \tilde{D}_{x_1, \alpha}^\sigma \tilde{\mathcal{G}}_\alpha,$$

187 in such a way that the o.d.e (13) becomes

$$(s^2 + \alpha^2 + k^2) \tilde{\mathcal{G}}_\alpha - \frac{d^2 \tilde{\mathcal{G}}_\alpha}{dX_1^2} = \delta(X_1 + h), \quad (14)$$

188 which leads to the following expression of $\tilde{\mathcal{G}}_\alpha$, for all $s > 0$,

$$\tilde{\mathcal{G}}_\alpha(X_1, k, s) = \frac{e^{-\sqrt{k^2 + s^2 + \alpha^2}|X_1 + h|}}{2\sqrt{k^2 + s^2 + \alpha^2}},$$

189 or equivalently for \tilde{G}_α ,

$$\tilde{G}_\alpha(x_1, k, s) = \frac{e^{-\sqrt{k^2 + s^2 + \alpha^2}\left|x_1 + h + \frac{\Sigma(x_1)}{\sqrt{s^2 + \alpha^2}}\right|}}{2\sqrt{k^2 + s^2 + \alpha^2}}.$$

190 It is now enough to observe that

$$\tilde{G}_\alpha(x_1, k, s) = \tilde{G}_{0,i}(x_1, k, \sqrt{s^2 + \alpha^2}). \quad (15)$$

191 However, $\tilde{G}_{0,i}(x_1, k, s)$ is nothing but the Fourier-Laplace transform of $G_i^{\sigma, \infty}$
 192 in space x_2 and time t , given in (7), which corresponds to the incident field in
 193 the dispersionless media (i.e. for $\alpha = 0$). Henceforth, the relation (12) of the
 194 theorem follows by Lemma 1 and injectivity of the Fourier transform. Finally,
 195 relations (10) and (11) follow directly by the image principle similarly as in [16]
 196 namely that the field reflected by the outer boundary of the PML is equivalent
 197 to the incident field of the image problem according to a Neumann boundary
 198 condition. The proof of the theorem is finished. ■

199 **Remark 1.** Observe that the perfect matching property of an infinite layer at
 200 $x_1 = 0$ can be seen directly in the expression of the total field $G_\alpha^{\sigma, \infty}(x, t) =$
 201 $G_{\alpha,i}^{\sigma, \infty}(x, t)$, for all $x_1 \in \mathbb{R}$, which means that no reflection holds at $x_1 = 0$ when
 202 the layer is infinite.

203 **Remark 2.** Actually, $G_{\alpha,i}^{\sigma, \infty}$ coincides on the left half-space $x_1 < 0$ with $G_{\alpha,i}^{0, \infty}$
 204 which corresponds to the Green's function associated to the KG equation in the
 205 whole space \mathbb{R}^2 with a source located in space at x_S . Its expression is well known
 206 in the literature cf. [23], and is given by

$$G_{\alpha,i}^{0, \infty}(x_1, x_2, t) = \frac{H(t - r(x))}{2\pi\sqrt{t^2 - r(x)^2}} \cos\left(\alpha\sqrt{t^2 - r(x)^2}\right). \quad (16)$$

207 In fact, one can also get it from the non-dispersive solution $G_{0,i}^{0, \infty}$ by applying
 208 Lemma 1.

209 **4. Error estimates and stability result**

210 We consider the solution $u_\alpha^{\sigma,L}$ of Problem (5) as an approximation of the
 211 solution $u_\alpha (= u_\alpha^{0,\infty})$ of the dispersive wave equation in the whole space:

$$\begin{cases} \text{Find } u_\alpha : \mathbb{R}^2 \times \mathbb{R}_+ \rightarrow \mathbb{R}, \text{ null for } t < 0, \\ \left(\frac{\partial^2}{\partial t^2} + \alpha^2 \right) u_\alpha - \frac{\partial^2 u_\alpha}{\partial x_1^2} - \frac{\partial^2 u_\alpha}{\partial x_2^2} = \delta(x - x_S) f(t), \end{cases} \quad (17)$$

Notice that $u_\alpha^{0,\infty}$ is nothing but the restriction of $u_\alpha^{\sigma,\infty}$ to the left half-space $\mathbb{R}_-^2 = \mathbb{R}_- \times \mathbb{R}$. We will give thus a time-domain analysis of the error

$$e_\alpha^{\sigma,L} = u_\alpha^{\sigma,L} - u_\alpha$$

212 w.r.t. to the parameters σ , L , h and α .

213 **Remark 3.** *The result (12) in Theorem 1 also applies for the total field, i.e.,*
 214 *one has for $G_\alpha^{\sigma,L}$ the same representation formula*

$$G_\alpha^{\sigma,L}(x, t) = G^{\sigma,L}(x, t) - \alpha \int_0^t G^{\sigma,L}\left(x, \sqrt{t^2 - z^2}\right) J_1(\alpha z) dz, \quad (18)$$

215 *which actually means that the field can be decomposed into two parts: the first*
 216 *one $G^{\sigma,L}(x, t)$ that is specific to a purely non-dispersive wave and the second*
 217 *one that is proportional to α and carries the dispersion when $\alpha \neq 0$.*

218 We deduce that analytical solution of Problem (5) can be obtained (for
 219 a regular source term $f(t)$) by a convolution in time in the sense of Laplace
 220 transform as follows:

$$u_\alpha^{\sigma,L}(x, t) = \int_0^{+\infty} G_\alpha^{\sigma,L}(x, \tau) f(t - \tau) d\tau.$$

221 Following Remark 3 and using the representation formula (18), it follows that
 222 the analytical solution $u_\alpha^{\sigma,L}(x, t)$ admits also a similar representation, i.e.,

$$u_\alpha^{\sigma,L}(x, t) = u^{\sigma,L}(x, t) - \alpha \int_0^t u^{\sigma,L}\left(x, \sqrt{t^2 - z^2}\right) J_1(\alpha z) dz, \quad (19)$$

223 which implies also that the same happens for the error function $e_\alpha^{\sigma,L}(x, t)$, i.e.

$$e_\alpha^{\sigma,L}(x, t) = e^{\sigma,L}(x, t) - \alpha \int_0^t e^{\sigma,L}\left(x, \sqrt{t^2 - z^2}\right) J_1(\alpha z) dz. \quad (20)$$

224 Here, $e^{\sigma,L}(x, t)$ is the error (or reflected field) without dispersion that has been
 225 fully studied in [16, Theorem 4]. After having redefined the time function $\Phi(t)$,

226 null for $t < 2L + h$, by:

$$\Phi(t) = \begin{cases} 0 & \text{if } t \leq 2L + h, \\ \ln \left(\frac{t + \sqrt{t^2 - (2L + h)^2}}{2L + h} \right) & \text{if } 2L + h < t \leq 2L + h + T, \\ \ln \left(\frac{t + \sqrt{t^2 - (t - T)^2}}{(t - T)} \right) & \text{if } t > 2L + h + T, \end{cases} \quad (21)$$

227 we recall that this error is bounded by

$$\|e^{\sigma, L}(\cdot, t)\|_{L^\infty(\mathbb{R}_-^2)} \leq \frac{1}{2} e^{-2\Sigma(L)\frac{2L+h}{t}} \Phi(t) \|f\|_{L^\infty}, \quad (22)$$

228 in such a way that for $T < \infty$, $\Phi(t)$ behaves for large t as $\mathcal{O}(\sqrt{2T/t})$ and
 229 $e^{\sigma, L}(\cdot, t)$ converges uniformly to 0 as t tends to $+\infty$, for all σ, L and h .

230 One can show that Φ is a positive and continuous function increasing for $2L + h <$
 231 $t < 2L + h + T$ and decreasing for $t > 2L + h + T$, hence $\Phi(t)$ reaches its maximum
 232 at $t = 2L + h + T$, i.e.

$$\max_{t \geq 0} \Phi(t) = \Phi_{max} = \Phi(2L + h + T) \quad (23)$$

233 The following Lemma gives uniform bound of an oscillating integral useful for
 234 the error estimate in the dispersive case, i.e. when α is non zero.

235 **Lemma 2.** *Let $\Phi(t)$ given by (21), then*

$$\alpha \int_0^t \Phi(\sqrt{t^2 - z^2}) |J_1(\alpha z)| dz \leq M(t) \sqrt{2\alpha},$$

236 where

$$M(t) = \begin{cases} 0 & \text{if } t \leq 2L + h, \\ T_0 \Phi_{max} & \text{if } 2L + h < t \leq 2L + h + 2T, \\ T_0 \Phi_{max} + 12\sqrt{T} \left(1 + 2\sqrt{\frac{T}{t}} \right) & \text{if } t > 2L + h + 2T, \end{cases}$$

237 Φ_{max} is given by (23) and $T_0 > 0$ is defined by

$$T_0 = 2 \left((2L + h + 2T)^2 - (2L + h)^2 \right)^{\frac{1}{4}}.$$

238 **Proof.** With the help of the change of variable $z = \sqrt{t^2 - x^2}$,

$$\alpha \int_0^t \Phi(\sqrt{t^2 - z^2}) |J_1(\alpha z)| dz = \alpha \int_0^t \Phi(x) \frac{x}{\sqrt{t^2 - x^2}} \left| J_1(\alpha \sqrt{t^2 - x^2}) \right| dx,$$

239 and by the following Bessel's function property, cf. [22]: the fact that for $\alpha > 0$
 240 and for all $z > 0$,

$$|J_1(\alpha z)| \leq \sqrt{\frac{2}{\alpha z}}, \quad (24)$$

241 one obtains the inequality

$$\alpha \int_0^t \Phi(x) \frac{x}{\sqrt{t^2 - x^2}} \left| J_1\left(\alpha \sqrt{t^2 - x^2}\right) \right| dx \leq \sqrt{2\alpha} \int_0^t \Phi(x) \frac{x}{(t^2 - x^2)^{\frac{3}{4}}} dx. \quad (25)$$

Henceforth, if $t \leq 2L + h$ then by definition $\Phi(x) = 0$ for all $x \in (0, t)$ and the r.h.s. of (25) is zero. Moreover, if $2L + h < t \leq 2L + h + 2T$ then one has

$$\begin{aligned} r.h.s.(25) &= \sqrt{2\alpha} \int_{2L+h}^t \Phi(x) \frac{x}{(t^2 - x^2)^{\frac{3}{4}}} dx, \\ &\leq \sqrt{2\alpha} \max_x \Phi(x) \int_{2L+h}^{2L+h+2T} \frac{x}{(t^2 - x^2)^{\frac{3}{4}}} dx = \sqrt{2\alpha} \Phi_{max} T_0. \end{aligned}$$

Furthermore, if $t > 2L + h + 2T$ then with the help of the standard inequality : $\log Z \leq Z - 1$ which holds for all $Z \geq 1$, one can write

$$\begin{aligned} \Phi(x) &= \ln \left(\frac{x + \sqrt{x^2 - (x - T)^2}}{(x - T)} \right) \leq \frac{T + \sqrt{T(2x - T)}}{x - T} \\ &\leq \frac{T + \sqrt{T(2x - 2T + T)}}{x - T} \\ &\leq \frac{2T}{x - T} + \sqrt{\frac{2T}{x - T}}. \end{aligned}$$

242 Hence, if $x > 2L + h + 2T$ then $x > 2T$ which yields $x - T > x/2$ and consequently
 243 the following estimate holds:

$$\Phi(x) \leq \frac{4T}{x} + \sqrt{\frac{4T}{x}}, \quad \forall x \in (2L + h + 2T, t).$$

One concludes that

$$\int_{2L+h+2T}^t \Phi(x) \frac{x}{(t^2 - x^2)^{\frac{3}{4}}} dx \leq \int_0^t \frac{4T + 2\sqrt{T}x}{(t^2 - x^2)^{\frac{3}{4}}} dx. \quad (26)$$

244 On the other hand, using a change of variable $x = t\sqrt{z}$, one has using the
 245 definition of the Euler integral of the first kind

$$\beta(u, v) = \int_0^1 z^{u-1} (1 - z)^{v-1} dz,$$

which is defined for $\Re(u) > 0$ and $\Re(v) > 0$,

$$\begin{aligned} \int_0^t x^\lambda (t^2 - x^2)^\mu dx &= t^{\lambda+2\mu+1} \int_0^1 z^{\frac{\lambda-1}{2}} (1-z)^\mu dz \\ &= t^{\lambda+2\mu+1} \beta\left(\frac{\lambda+1}{2}, \mu+1\right), \end{aligned}$$

which in turn exists for $\Re(\lambda) > -1$ and $\Re(\mu) > -1$. Henceforth, the r.h.s. of (26) can be calculated, with the help of the previous identity, as follows:

$$\begin{aligned} \int_0^t \frac{4T + 2\sqrt{T}x}{(t^2 - x^2)^{\frac{3}{4}}} dx &= \int_0^t \frac{4T}{(t^2 - x^2)^{\frac{3}{4}}} dx + \int_0^t \frac{2\sqrt{T}x}{(t^2 - x^2)^{\frac{3}{4}}} dx, \\ &= 4T \int_0^t x^0 (t^2 - x^2)^{-\frac{3}{4}} dx + 2\sqrt{T} \int_0^t x^{\frac{1}{2}} (t^2 - x^2)^{-\frac{3}{4}} dx, \\ &= 4T t^{-\frac{1}{2}} \beta\left(\frac{1}{2}, \frac{1}{4}\right) + 2\sqrt{T} t^0 \beta\left(\frac{3}{4}, \frac{1}{4}\right), \\ &\leq 12\sqrt{T} \left(2\sqrt{\frac{T}{t}} + 1\right), \end{aligned}$$

246 since one has

$$\beta\left(\frac{3}{4}, \frac{1}{4}\right) < \beta\left(\frac{1}{2}, \frac{1}{4}\right) < 6.$$

247 Thus, if $t > 2L + h + 2T$ then by the decomposition

$$\int_0^t = \int_0^{2L+h} + \int_{2L+h}^{2L+h+2T} + \int_{2L+h+2T}^t,$$

one concludes that

$$\alpha \int_0^t \Phi\left(\sqrt{t^2 - z^2}\right) |J_1(\alpha z)| dz \leq \left(T_0 \Phi_{max} + 12\sqrt{T} \left(1 + 2\sqrt{\frac{T}{t}}\right)\right) \sqrt{2\alpha}, \quad (27)$$

248 which ends the proof of the Lemma. ■

249 **Theorem 2.** For a regular source term $f(t)$ compactly supported in $[0, T]$, $T <$
 250 $+\infty$, the error $e_\alpha^{\sigma, L}(\cdot, t) = v_\alpha^{\sigma, L}(\cdot, t) - u_\alpha(\cdot, t)$ is null for $t < 2L + h$, and for all
 251 $t \geq 2L + h$ the following estimate holds:

$$\|e_\alpha^{\sigma, L}(\cdot, t)\|_{L^\infty(\mathbb{R}_-^2)} \leq \frac{1}{2} e^{-2\Sigma(L)\frac{2L+h}{t}} \|f\|_{L^\infty} \left(\Phi(t) + M(t)\sqrt{2\alpha}\right), \quad (28)$$

252 where $M(t)$ is defined in Lemma 2.

Proof. Thanks to Inequality (22) it will be enough to estimate the second term in the r.h.s. in the representation formula (20). So, one has again by Inequality (22):

$$\begin{aligned} \|e_{\alpha}^{\sigma,L}(\cdot, t) - e^{\sigma,L}(\cdot, t)\|_{L^{\infty}(\mathbb{R}^2)} &= \sup_{x \in \mathbb{R}^2} \left| \alpha \int_0^t e^{\sigma,L} \left(x, \sqrt{t^2 - z^2} \right) J_1(\alpha z) dz \right| \\ &\leq \frac{\alpha}{2} \|f\|_{L^{\infty}} \int_0^t e^{-2\Sigma(L) \frac{2L+h}{\sqrt{t^2 - z^2}}} \Phi \left(\sqrt{t^2 - z^2} \right) |J_1(\alpha z)| dz. \end{aligned} \quad (29)$$

253 With the help of the triangular inequality, one has

$$\|e_{\alpha}^{\sigma,L}(\cdot, t)\|_{L^{\infty}(\mathbb{R}^2)} \leq \|e_{\alpha}^{\sigma,L}(\cdot, t) - e^{\sigma,L}(\cdot, t)\|_{L^{\infty}(\mathbb{R}^2)} + \|e^{\sigma,L}(\cdot, t)\|_{L^{\infty}(\mathbb{R}^2)}.$$

254 Moreover,

$$\sup_{z \in (0, t)} e^{-2\Sigma(L) \frac{2L+h}{\sqrt{t^2 - z^2}}} = e^{-2\Sigma(L) \frac{2L+h}{t}},$$

255 then (22) implies that the r.h.s of (29) is bounded from above by

$$\frac{\alpha e^{-2\Sigma(L) \frac{2L+h}{t}} \|f\|_{L^{\infty}}}{2} \int_0^t \Phi \left(\sqrt{t^2 - z^2} \right) |J_1(\alpha z)| dz. \quad (30)$$

256 Henceforth, the proof of the theorem follows by Lemma 2 and Inequality (22).
257 In particular, the error is zero for $t < 2L + h$ since $\Phi(t) = M(t) = 0$ for all
258 $t < 2L + h$. ■

259 It should be pointed that the presence of the function $M(t)$ in the r.h.s. of the
260 estimate (28) can be interpreted as a result of stability only. More precisely, we
261 can see that for t large, $M(t)$ does not have the same asymptotic behavior as
262 $\Phi(t)$. Indeed, $M(t) = \sqrt{\alpha} \mathcal{O}(1)$ while $\Phi(t) = \mathcal{O}(t^{-1/2})$.

263 5. Localization and numerical application

264 The operator $D_{x_1, \alpha}^{\sigma}$ that appears in the PML change of variable (3) is non-
265 local. Therefore, we propose a localization technique at high frequencies simi-
266 larly to the ABC's methodology [17]. As an example, comparisons (numerical
267 and plane waves analysis) of the zeroth and first order Taylor approximations of
268 the square root $\sqrt{\partial_t^2 + \alpha^2}$ are feasible and will be sufficient to put in evidence
269 the effect of the dispersion parameter α .

270 5.1. Localization

271 The expression of the PML equation obtained in Section 2 is non-local since
272 a square root appears in the change of variable (3), which is far from being
273 practical in a numerical application. A standard zeroth-order approximation at
274 high frequencies can be used, just as usually done by the authors when dealing
275 with dispersive wave equation by taking (for example) simply $\alpha = 0$ in (3) to

276 obtain the standard form of $D_{x_1}^\sigma$ as given by (2), (cf. eg. [2, 5, 27]). Instead
 277 of that, we propose here a new family of PML's operators by a localization
 278 technique that can be based on a Taylor or any other asymptotic expansion
 279 (such as Padé's approximation) of the square root $\sqrt{s^2 + \alpha^2}$ at high frequencies
 280 (of a specific order). It is similar to those used in designing absorbing boundary
 281 conditions ([17, 18, 20, 15, 27]). At high frequencies $\alpha \ll s$, one can write

$$\sqrt{s^2 + \alpha^2} = s + \frac{1}{2}\alpha^2 s^{-1} + \mathcal{O}\left(\frac{\alpha}{s}\right)^4. \quad (31)$$

282 The computation of $\xi = D_{x_1, \alpha}^\sigma \phi$ can be done by inverting the operator corre-
 283 sponding to the symbol $\sqrt{s^2 + \alpha^2} + \sigma$ in the equation, i.e.,

$$\left(\sqrt{s^2 + \alpha^2} + \sigma\right) \xi = \sqrt{s^2 + \alpha^2} \frac{d}{dx_1} \phi, \quad (32)$$

284 and at high frequencies $\alpha \ll s$, the square root $\sqrt{s^2 + \alpha^2}$ may be replaced by
 285 dropping the highest order terms in the expansion (31) in such a way that (32)
 286 can be approximated by the equation

$$\left(s + \frac{1}{2}\alpha^2 s^{-1} + \sigma\right) \xi = \left(s + \frac{1}{2}\alpha^2 s^{-1}\right) \frac{d}{dx_1} \phi,$$

287 and, which up to a multiplication by s , gives

$$\left(s^2 + \frac{1}{2}\alpha^2 + \sigma s\right) \xi = \left(s^2 + \frac{1}{2}\alpha^2\right) \frac{d}{dx_1} \phi.$$

288 Hence, the localization of $D_{x_1, \alpha}^\sigma$ (by a Taylor approximation) can be done by
 289 solving a Cauchy problem as follows:

$$\begin{cases} \left(\frac{\partial^2}{\partial t^2} + \frac{1}{2}\alpha^2 + \sigma \frac{\partial}{\partial t}\right) \xi(x, t) = \left(\frac{\partial^2}{\partial t^2} + \frac{1}{2}\alpha^2\right) \frac{\partial}{\partial x_1} \phi(x, t), & x_1 > 0, \\ \frac{\partial}{\partial t} \xi(x, t) \Big|_{t=0} = 0, \end{cases} \quad (33)$$

290 together with the perfect matching condition

$$\xi(x, t) \Big|_{x_1=0^+} = \frac{\partial}{\partial x_1} \phi(x, t) \Big|_{x_1=0^-}$$

291 and the fact that the auxiliary variable ξ lives only in the PML layer $x_1 > 0$,
 292 i.e.,

$$\xi(x, t) = 0, \quad x_1 < 0.$$

293 We will call the Taylor approximation given by the PML equation in the form
 294 (33) the α -PML in the numerical results thereafter. Notice that in the case
 295 of infinite layers, both the standard PML and α -PML are by construction

296 perfectly matched at the interface $x_1 = 0$. In fact, to each one corresponds the
 297 following complex change of variable:

$$X_1(x_1, s) = x_1 + \frac{1}{s} \int_0^{x_1} \sigma(x) dx, \quad (34)$$

298 for the standard, and

$$X_1(x_1, s) = x_1 + \frac{1}{s + \frac{1}{2}\alpha^2 s^{-1}} \int_0^{x_1} \sigma(x) dx,$$

299 for the α -PML. Note also that when a finite layer of width L is used one has
 300 to add for example a homogeneous Neumann boundary condition on ξ in order
 301 to close the equations. Let us point out that a standard PML formulation will
 302 correspond to a zeroth order approximation in (32), i.e., by taking $\alpha = 0$ in
 303 (33).

304 5.2. Plane waves analysis

305 The homogeneous non-dispersive wave equation ($\alpha = 0$) admits outgoing
 306 plane wave solutions in the direction of increasing x_1 of the following form

$$U = e^{i\omega t - ik_1 x_1 + ik_2 x_2}, \quad \frac{k_1}{\omega} > 0, \quad (35)$$

307 where the time and space frequencies are related by the dispersion relation
 308 $\omega^2 - k_1^2 - k_2^2 = 0$.

It is well known that, when considering a finite layer (corresponding to the
 standard PML change of variable (34) with $s = i\omega$) of width L with homoge-
 neous Neumann boundary condition at $x_1 = L$, then the image principle allows
 one to obtain through simple reflection a plane wave solution of the form

$$\begin{aligned} u(X, t) &= U(X, t) + U(X^*, t), \\ &= e^{i(\omega t - k_1 X_1 + k_2 x_2)} + e^{i(\omega t - k_1(2L - X_1) + k_2 x_2)}, \\ &= e^{i(\omega t - k_1 X_1 + k_2 x_2)} + e^{i(\omega t - k_1(2L - X_1) + k_2 x_2)}, \\ &= e^{i(\omega t - k_1 x_1 + k_2 x_2)} e^{-\frac{k_1}{\omega} \int_0^{x_1} \sigma(\xi) d\xi} + e^{i(\omega t - k_1(2L - x_1) + k_2 x_2)} e^{-\frac{k_1}{\omega} \int_0^{2L - x_1} \sigma(\xi) d\xi}, \end{aligned}$$

309 so that in the region $x < 0$ the solution becomes

$$u(x, t) = e^{i(\omega t - k_1 x_1 + k_2 x_2)} + R_\sigma e^{i(\omega t + k_1 x_1 + k_2 x_2)},$$

310 where

$$R_\sigma = e^{-\frac{k_1}{\omega} \int_0^{2L - x_1} \sigma(\xi) d\xi} e^{-2ik_1 L}.$$

Moreover, one has for $x_1 < 0$,

$$\int_0^{2L - x_1} \sigma(\xi) d\xi = 2 \int_0^L \sigma(\xi) d\xi$$

311 since σ was extended symmetrically w.r.t. the line $x_1 = L$. We thus find the
 312 reflection coefficient at the interface $x_1 = 0$:

$$R_\sigma = e^{-2\frac{k_1}{\omega} \int_0^L \sigma(\xi) d\xi} \times e^{-2ik_1L}, \quad (36)$$

313 where the first term in the r.h.s. of (36) is associated with absorption and the
 314 second represents a phase shift.

Similarly to the change of Laplace variable s by $\sqrt{s^2 + \alpha^2}$ that we used in Section 3, we propose to analyze the reflectivity of the non-local PML for the KG equation as follows. The frequency change of variable ω by $\sqrt{\omega^2 - \alpha^2}$ in (35) transforms the plane wave solution of the non-dispersive wave equation to a plane wave solution of the KG equation of the form

$$U_\alpha = e^{i\sqrt{\omega^2 - \alpha^2}t - ik_1x_1 + ik_2x_2},$$

315 in such a way that the expression of the reflection coefficient of the finite width
 316 non-local PML at the interface $x_1 = 0$ writes as

$$R_{\sigma,\alpha} = e^{-2\frac{k_1}{\sqrt{\omega^2 - \alpha^2}} \int_0^L \sigma(\xi) d\xi} \times e^{-2ik_1L}. \quad (37)$$

317 Henceforth, a Taylor series of the square root $\sqrt{\omega^2 - \alpha^2}$ at high frequencies
 318 ($\alpha \ll \omega$) will give the following approximations of $R_{\sigma,\alpha}$, at increasing orders:

$$R_{\sigma,\alpha}^{(0)} = e^{-2\frac{k_1}{\omega} \int_0^L \sigma(\xi) d\xi} \times e^{-2ik_1L},$$

319

$$R_{\sigma,\alpha}^{(1)} = e^{-2\frac{k_1}{\omega - \frac{\alpha^2}{\omega}} \int_0^L \sigma(\xi) d\xi} \times e^{-2ik_1L}, \dots$$

320 These coefficients correspond exactly and respectively to the coefficients of reflection
 321 at $x_1 = 0$ of the standard (0-PML) and the α -PML, ..., associated
 322 with the KG equation. As a result, we have for all $\alpha > 0$ and k_1, ω such that
 323 $\omega \geq \alpha$ and $k_1/\omega > 0$,

$$\left| R_{\sigma,\alpha}^{(1)} \right| < \left| R_{\sigma,\alpha}^{(0)} \right|,$$

324 which means that the α -PML improves the standard PML. Better yet, the
 325 improvement is optimal at long waves which have frequencies close to α . Indeed,
 326 one has the ratio

$$\left| \frac{R_{\sigma,\alpha}^{(1)}}{R_{\sigma,\alpha}^{(0)}} \right| = e^{-2\frac{k_1}{\omega} \frac{\alpha^2}{2\omega^2 - \alpha^2} \int_0^L \sigma(\xi) d\xi} \quad (38)$$

327 that is increasing w.r.t. $\omega \in [\alpha, +\infty[$ and henceforth is minimal at $\omega = \alpha$. We
 328 conclude this by remarking that, at least for plane waves, α -PML performs
 329 better than the standard one and better still for long waves, i.e., in the vicinity
 330 of the cut-off frequency α . Otherwise, the two methods (standard and α -PMLs)
 331 are virtually identical for short waves (high frequencies $\omega \gg \alpha$) or in general for
 332 weakly dispersive waves ($\alpha \simeq 0$).

333 **Remark 4.** *The localization process in this section is based on the high fre-*
 334 *quency/short wave ($s \gg \alpha$) assumption, and yet the new formulation is aimed*
 335 *to deal with the long waves (s close to α). In fact, the localization is expected to*
 336 *be less accurate for the more dispersive waves if one uses only few terms in the*
 337 *Taylor expansion. Other asymptotic expansion such as Padé's approximation of*
 338 *the square root $\sqrt{s^2 + \alpha^2}$ at high frequencies may actually performs better with*
 339 *a slightly higher cost resulting from the quasi-localization by rational fractions.*

340

341 **Remark 5.** *Currently there is no reason to believe in the long-time stability of*
 342 *either 0-PML or α -PML in terms of analytical solutions. Nevertheless, a plane*
 343 *wave analysis with an infinite layer based on the slowness curves can be carried*
 344 *out without difficulty in order to show their stability at least for exponential*
 345 *modes as in [5, 6, 7].*

346 5.3. Numerical examples

347 In what follows, we will present results for both the standard (0-PML)
 348 and the α -PML in order to discuss the effect of taking or not α into account
 for the precision of computations. The numerical solutions are obtained by a

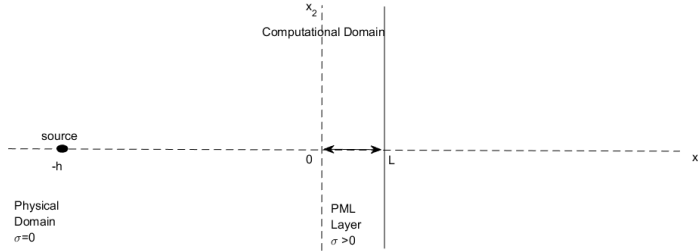


Figure 4: Configuration of the computational and physical domains and the vertical layer of width L . The source lies in the physical media outside the interface.

349

350 finite difference time-domain code (FDTD) based on a standard central finite
 351 difference scheme of leap-frog type, second order accurate in space and time,
 352 where the source function is a truncated first derivative of a Gaussian :

$$f(t) = \frac{d}{dt} \left\{ e^{-2\pi f_0(t-t_0)^2} \right\} H(2t_0 - t), \quad f_0 = 10, \quad t_0 = \frac{1}{f_0}.$$

353 It produces for $c = 1$ a wavelength $\lambda = c/f_0 = 0.1$. The space step size Δx is
 354 chosen equal in both direction x_1 and x_2 , such that $\Delta x = \lambda/16$, i.e., 16 points
 355 per wavelength, with a CFL condition such that $c\Delta t/\Delta x = 0.5$.

356 Let us point out that a layer in the x_2 direction (the horizontal layer) can be
 357 constructed straightforwardly by symmetry from the x_1 direction (the vertical

358 layer). The corner layers are constructed side by side of the vertical and hori-
 359 zontal ones without any special care as is commonly used in PML techniques for
 360 the wave equation. We used natural transmission conditions and the numerical
 361 results show no reflection at the interfaces separating the two layers. In order
 362 to perform a long time simulation, we consider a rectangular physical domain
 363 $[-60\Delta x, 0] \times [-30\Delta x, 30\Delta x]$ completely surrounded by vertical and horizontal
 364 layers of same width $L = 20\Delta x$ and the point source is assumed located at
 365 $X_S = (-30\Delta x, 0)$. Our interest is focused only on the behaviour of the right
 366 vertical layer $0 < x_1 < L$ (cf. Figure 4) since it will be adequate to conclude
 367 later. The damping function $\sigma(x_1) = \sigma_{max}x_1^2/L$ is chosen quadratic with an
 368 empirical maximum value $\sigma_{max} = 48$. An observation point x_R (the receiver)
 369 at normal incidence is chosen on the x_1 -axis at left two-points away from the
 370 interface between physical domain and PML layer.

371 - *Comparison of FDTD and convolution analytical solutions*

372 Dispersion appears at very long periods in time, which results in an ad-
 373 justment of long waves towards the inertial oscillations of frequencies α . We
 374 have thus computed the analytical solution $u_\alpha(x_R, t)$ via the Maple software
 375 by calculating oscillating convolution integrals involving a cosine function (cf.
 376 Eq.(16)) to match with the finite difference reference solution. Figures 5 and
 377 6 show the long waves adjustment of the analytical solution computed by the
 378 software Maple with $\alpha = 0.1f_0$ (weak dispersion) and with $\alpha = 0.9f_0$ (strong
 379 dispersion) respectively. We have also computed the analytical (or reference)
 380 solution by the finite difference code on a much larger computational domain
 381 $[-500\Delta x, 0] \times [-250\Delta x, 250\Delta x]$ by setting $\sigma = 0$ and where the simulation time
 382 $T_R = 900\Delta t$ is chosen so that the reflected wave will not have reached the outer
 383 boundary yet. Figures 7 and 8 show comparisons for short waves adjustment of
 384 the analytical solution computed by the software Maple and the FDTD code,
 385 where we have set $\alpha = 0.1f_0$ for weak dispersion and $\alpha = 0.9f_0$ for strong dis-
 386 persion respectively. The two solutions (convolution and FDTD) are in good
 387 agreement in each case. Figures 9 and 10 show relative error incurred by the
 388 FDTD code w.r.t. the convolution integral formula to obtain analytical solution
 389 respectively for weak dispersion ($\alpha = 0.1f_0$) and strong dispersion ($\alpha = 0.9f_0$).
 390

391 From now on, and since very long time simulation is needed later for long
 392 waves, we will use the convolution solution as the reference analytical solution
 393 for the error analysis of both the standard and α -PML.

394 - *Short waves analysis of PMLs*

395 We will first make a comparison between the standard PML and the α -PML
 396 during the passage of the short wave, say for $t \in [0, 900\Delta t]$, by computing the
 397 relative error produced by each method w.r.t. the analytical solution. Denoting
 398 by $u_\alpha(x_R, t)$ the PML (standard or α -) solution, the relative error is defined
 399 by

$$E_\alpha^{\sigma, L}(x_R, t) = \frac{|u_\alpha(x_R, t) - u_{ref}(x_R, t)|}{\max_{0 \leq t \leq 900\Delta t} |u_{ref}(x_R, t)|}$$

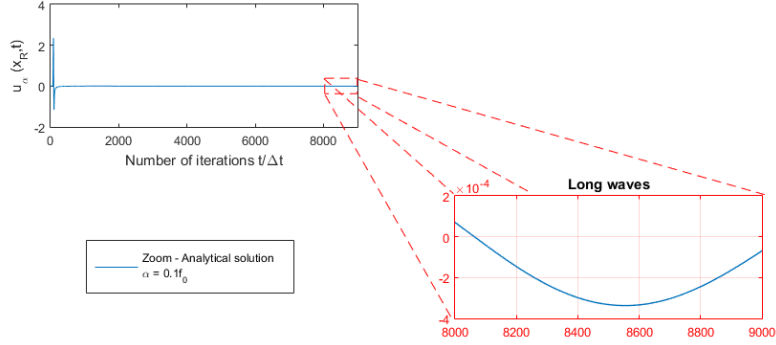


Figure 5: Weak dispersion: Zoom close to inertial oscillations adjustment of the analytical solution computed by Maple with $\alpha = 0.1f_0$.

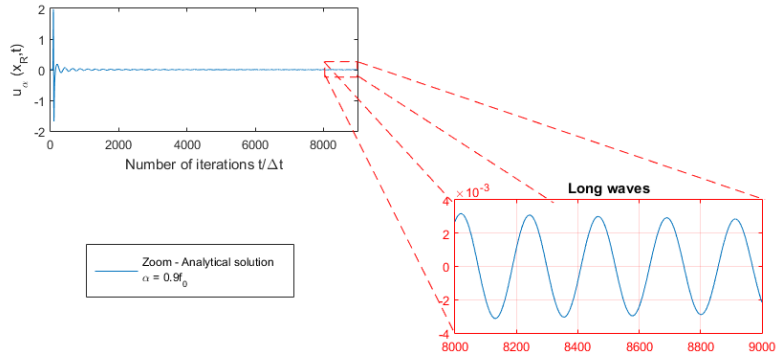


Figure 6: Strong dispersion: Zoom close to inertial oscillations adjustment of the analytical solution computed by Maple with $\alpha = 0.9f_0$.

400 and it is calculated for $\alpha = 0.1f_0$ (weak dispersion) and $\alpha = 0.9f_0$ (strong
 401 dispersion) respectively. In the two cases we have tested the standard PML and
 402 the α -PML. Results for short waves are shown in Figures 11 and 12 respectively.
 403 According to the tolerance obtained in Figures 9 and 10 between the Convolution
 404 and FDTD analytical solutions, both standard PML and α -PML performs
 405 with the same precision. One can conclude that, at least for short waves, one
 406 can continue using the standard PML without having recourse to the second
 407 method (α -PML), as it is done in the literature for dispersive problems (cf. eg.
 408 [2, 5, 27]).

409 - *Long waves analysis of PMLs*

410 In order to highlight the positive contribution of α -PML w.r.t. the standard,
 411 we will focus on the long time periods (for example $t \geq 900\Delta t$) during which
 412 long waves adjustment occurs (in particular the case of a strong dispersion

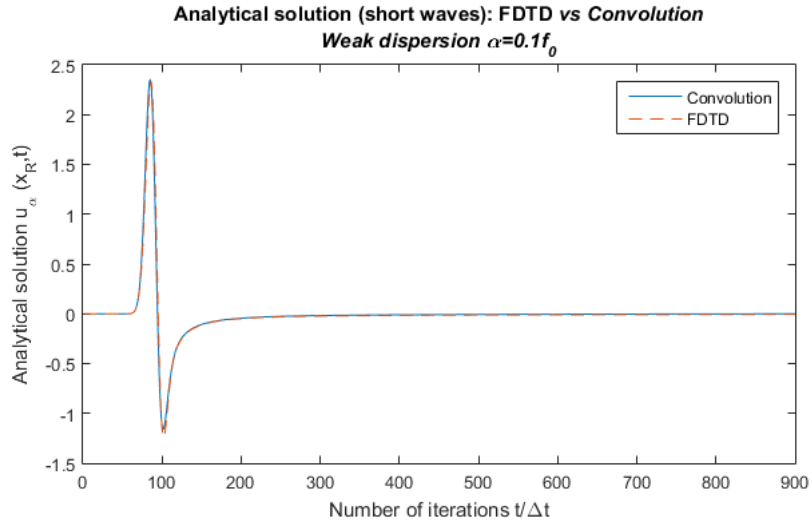


Figure 7: Weak dispersion $\alpha = 0.1f_0$: Convolution vs FDTD

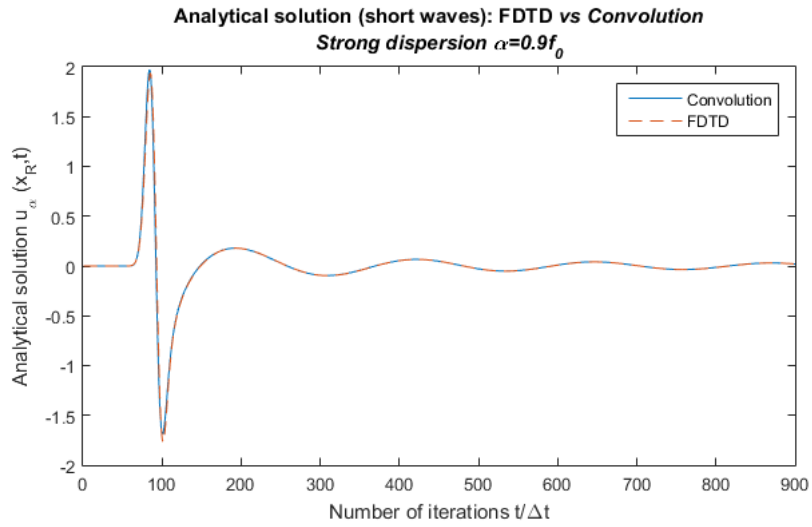


Figure 8: Strong dispersion $\alpha = 0.9f_0$: Convolution vs FDTD

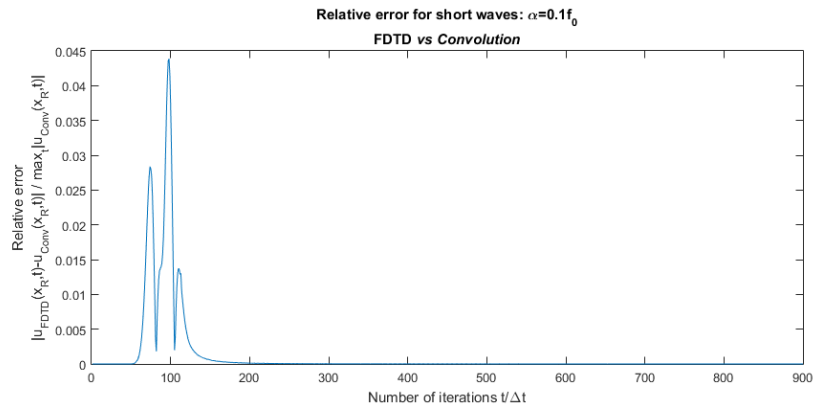


Figure 9: Relative error for short waves for $\alpha = 0.1f_0$: FDTD *vs* Convolution solution.

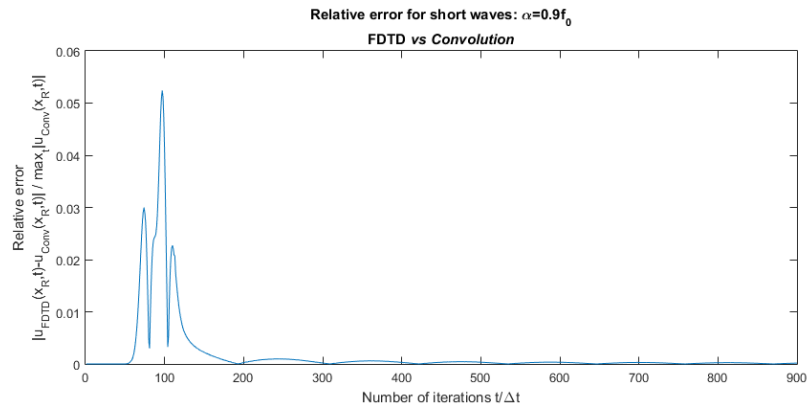


Figure 10: Relative error for short waves for $\alpha = 0.9f_0$: FDTD *vs* Convolution solution.

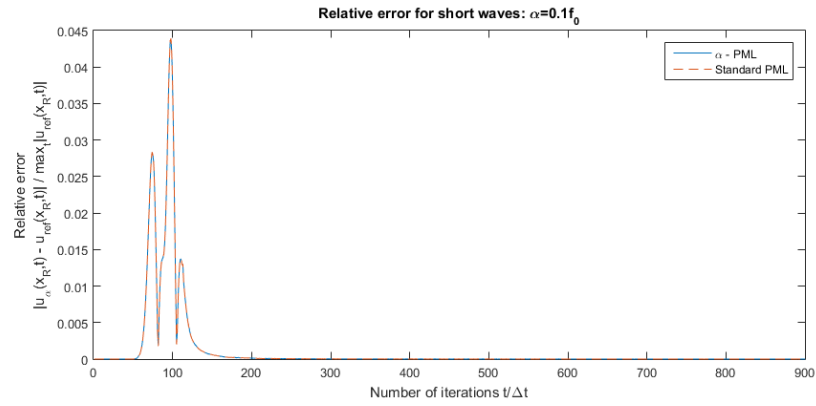


Figure 11: Weak dispersion, $\alpha = 0.1f_0$: relative error of standard PML and α -PML w.r.t. analytical solution.

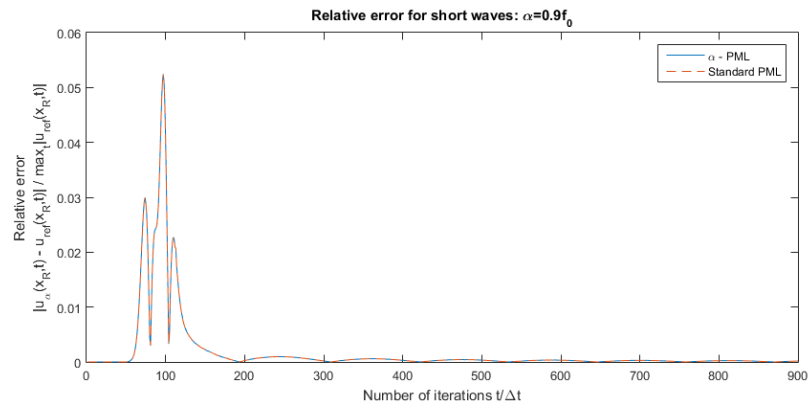


Figure 12: Strong dispersion, $\alpha = 0.9f_0$: relative error of standard PML and α -PML w.r.t. analytical solution.

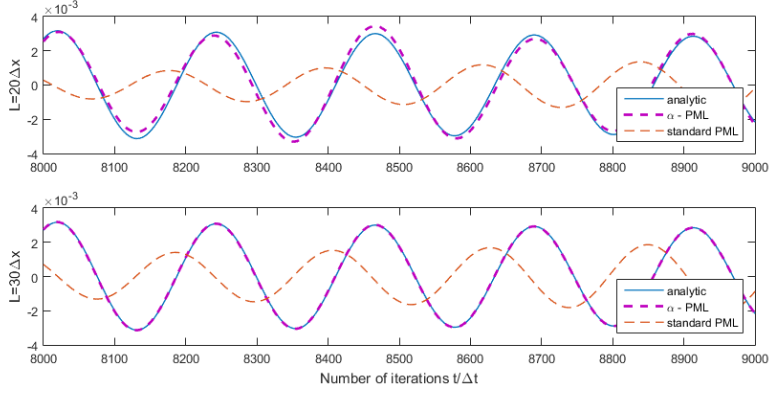


Figure 13: Comparison of standard and α -PMLs for long waves.

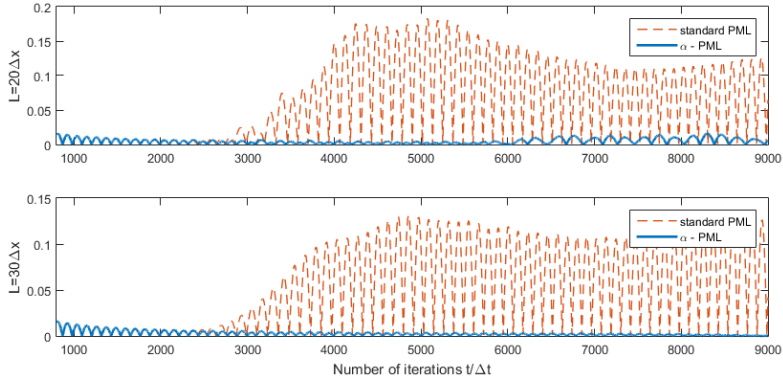


Figure 14: Relative error of standard and α -PMLs for long waves.

413 $\alpha = 0.9f_0$). The relative error produced by each method w.r.t. the analytical
 414 solution is defined now by

$$E_{\alpha}^{\sigma,L}(x_R, t) = \frac{|u_{\alpha}(x_R, t) - u_{ref}(x_R, t)|}{\max_{900\Delta t \leq t \leq 9000\Delta t} |u_{ref}(x_R, t)|},$$

415 where $u_{\alpha}(x_R, t)$ denotes now the PML (standard or α -) solution. We have
 416 tested two cases of the width of the PML layer, $L = 20\Delta x$ and $L = 30\Delta x$ for
 417 each method respectively. Figure 14 shows, for a last sample of time interval
 418 $t \geq 800\Delta t$, a comparison of long waves adjustment obtained by the standard
 419 and α -PML *vs* the analytical solution, top picture with $L = 20\Delta x$ and bottom
 420 with $L = 30\Delta x$. We observe remarkably good agreement of the α -PML
 421 solution with the analytical one while the one given by the standard PML remains visibly
 422 far from this adjustment. Even more precisely, in Figure 14 we observe that
 423 the relative error incurred by the α -PML is much less significant than that
 424 produced by the standard for $L = 20\Delta x$ at top picture. Better yet at bottom, it

425 is even decreasing in time for $L = 30\Delta x$, whereas that produced by the standard
 426 remains just bounded and above all relatively significant by comparison with
 427 the α -PML. This is also in good agreement with the behaviour for ω close to
 428 α of the ratio of reflection coefficients given by (38) in the plane wave analysis
 429 above.

430 6. Conclusion

- 431 • As a principal consequence of Theorem 2, the error is not affected by the
 432 dispersion term α at a fixed time $t > 0$. Therefore, the design of PML
 433 for dispersive waves may be the same as for the non-dispersive case for
 434 short time simulation and particularly for short waves. More precisely,
 435 at fixed time t this error is affected only by the average absorption rate
 436 $\bar{\sigma} = \Sigma(L)/L$, the width of the layer L and the location of the source
 437 h while it converges spectrally in the L^∞ norm to 0 when one of these
 438 parameters increases.
- 439 • Specifically, we do not observe the same behaviour in long time, that is to
 440 say, for fixed $T < \infty$ the error behaves for large t as

$$\sqrt{\frac{2T}{t}} + \mathcal{O}(\sqrt{\alpha})$$

441 and does not necessarily converge uniformly to 0 as t tends to $+\infty$ for all
 442 $\bar{\sigma}, L$ and h . This is the main difference (or loss in precision) w.r.t. the
 443 non-dispersive case ($\alpha = 0$). However and fortunately, the property of
 444 long time stability is conserved since the error remains bounded as t goes
 445 to $+\infty$.

- 446 • This technique can in particular be used to study the shallow water equa-
 447 tions with rotation in order to take into account the effect of the Coriolis
 448 force on the behaviour of the absorbing layers.
- 449 • Advective Klein-Gordon equation with a parallel mean flow can be ana-
 450 lyzed in a very similar way in comparison with the time domain analysis
 451 presented for advective acoustics in [16], the same changes of variables can
 452 be used as in [21, 5] in order to get rid of the moving referential. However,
 453 this sill be not yet obvious at an oblique mean flow.
- 454 • The idea of localization proposed in Section 5 is very standard but it opens
 455 a wide variety of possibilities in designing absorbing boundary conditions
 456 combined with PMLs using other techniques of approximating the square
 457 root $\sqrt{s^2 + \alpha^2}$ appearing in $D_{x_1, \alpha}^\sigma$.

458 References

- 459 [1] S. Abarbanel and D. Gottlieb. A mathematical analysis of the PML
 460 method, J. Comput. Phys. 134 (2) (1997) 357–363.

- 461 [2] S. Abarbanel, D. Stanescu, and M. Hussaini. Unsplit Variables Perfectly
462 Matched Layers for the Shallow Water Equations with Coriolis Forces,
463 Computational Geosciences (2003) 7–275.
- 464 [3] M. Abramowitz, and I. Stegun. Handbook of Mathematical Functions with
465 Formulas, Graphs, and Mathematical Tables, edited by M. Abramowitz
466 and I. Stegun (Dover, New York, 1964).
- 467 [4] Arthur Erdelyi. *Tables of integral transforms*. McGraw-Hill Inc.,US. Vol.1.
468 (1954). Pages 410.
- 469 [5] H. Barucq, J. Diaz, and M. Tlemcani. New absorbing layers conditions for
470 short water waves, J. of Comp. Phys., 229 (1) (2010) 58–72.
- 471 [6] E. Bécache, S. Fauqueux, and P. Joly, Stability of perfectly matched layers,
472 group velocities and anisotropic waves, J. Comput. Phys. 188 (2) (2003)
473 399–433.
- 474 [7] E. Bécache, P. Joly, and V. Vinoles. On the analysis of perfectly matched
475 layers for a class of dispersive media and application to negative index
476 metamaterials. Math. Comp. 87 (2018), no. 314, 2775–2810.
- 477 [8] J.-P. Bérenger. A perfectly matched layer for the absorption of electromag-
478 netic waves, J. Comput. Phys. 114 (1994) 185–200.
- 479 [9] J. P. Bérenger. Three-dimensional perfectly matched layer for the absorp-
480 tion of electromagnetic waves, J. of Comp. Phys., 127 (1996) 363–379.
- 481 [10] L. Cagniard. Reflection and refraction of progressive seismic waves, Mc-
482 GrawHill, (1962).
- 483 [11] F. Collino and P. Monk. The Perfectly Matched Layer in curvilinear coor-
484 dinates, SIAM J. Scient. Comp. 164 (1998) 157–171.
- 485 [12] F. Collino and C. Tsogka. Application of the pml absorbing layer model
486 to the linear elastodynamic problem in anisotropic heterogeneous media,
487 Geophysics 66 (1) (2001) 294–307.
- 488 [13] A. T. de Hoop. The surface line source problem, Appl. Sci. Res. B 8 (1959)
489 349–356.
- 490 [14] A. T. de Hoop, P. Van den Berg, and F. Remis. Analytic time-domain per-
491 formance analysis of absorbing boundary conditions and perfectly matched
492 layers, in: Proc. IEEE Antennas and Propagation Society International
493 Symposium, Vol. 4, (2001), pp. 502–505.
- 494 [15] J. Diaz and P. Joly. An Analysis of Higher Order Boundary Conditions for
495 the Wave Equation *SIAM J. Appl. Math.*, 65(5): 1547–1575, 2005.
- 496 [16] J. Diaz and P. Joly. A time domain analysis of PML models in acoustics.
497 Comput. Methods Appl. Mech. Engrg. 195 (2006), no. 29-32, 3820–3853.

- 498 [17] B. Engquist and A. Majda. Radiation boundary conditions for acoustic and
499 elastic wave calculations, *Comm. Pure Appl. Math.* 32 (1979) 313-357.
- 500 [18] B. Engquist and A. Majda. Absorbing boundary conditions for the numer-
501 ical simulation of waves, *Math. Comp.* 31 (1997) 629-651.
- 502 [19] S. Fauqueux. Eléments finis mixtes spectraux et couches absorbantes par-
503 faitement adaptées pour la propagation d'ondes élastiques en régime tran-
504 sitoire, Ph.D. thesis, Université Paris IX (2003).
- 505 [20] D. Givoli and B. Neta. High-order nonreflecting boundary conditions for the
506 dispersive shallow water equations, *Journal of Computational and Applied*
507 *Mathematics* 158 (1) (2003) 49-60.
- 508 [21] F. Q. Hu. On absorbing boundary conditions for linearized euler equations
509 by a perfectly matched layer, *J. Comp. Phys.* (129) (1996) 201-219.
- 510 [22] A. YA. Olenko. Upper bound on $\sqrt{x}J_\nu(x)$ and its applications. *Integral*
511 *Transforms and Special Functions* Vol. 17, No. 6, June 2006, 455-467.
- 512 [23] Andrei D, Polyanin. *Handbook of linear partial differential equations for*
513 *engineers and scientists*. Boca Raton: Chapman & Hall/CRC, 2002.K.
- 514 [24] J. Pedlosky *Geophysical Fluid Dynamics*. Springer, New York, NY, 1987,
515 XIV, pages 710.
- 516 [25] K. Watanabe. Cagniard-de Hoop Technique, In: *Integral Transform Tech-*
517 *niques for Green's Function*. Lecture Notes in Applied and Computational
518 *Mechanics*, Springer, Cham, 76 (2015) 153-204.
- 519 [26] L. Zhao and A. C. Cangellaris. A General Approach for the Development of
520 Unsplit Field Time-Domain Implementations of Perfectly Matched Layers
521 for FDTD Grid Truncation, *IEEE Microwave and Guided Letters* 6 (5)
522 (1996) 209-211.
- 523 [27] Lancioni, Giovanni. Numerical comparison of high-order absorbing bound-
524 ary conditions and perfectly matched layers for a dispersive one-dimensional
525 medium. *Comput. Methods Appl. Mech. Engrg.* 209/212 (2012), 74-86.